

REACTIVE TRANSPORT MODELING USING A PARALLEL FULLY- COUPLED SIMULATOR BASED ON PRECONDITIONED JACOBIAN- FREE NEWTON-KRYLOV

Luanjing Guo^{*}, Chuan Lu^{*}, Hai Huang^{*} and Derek R. Gaston[†]

^{*} Energy and Environment Science & Technology, [†] Nuclear Science & Technology
Idaho National Laboratory
P.O. Box 1625, MS 2107
Idaho Falls, ID, 83415-2107 U.S.A.
e-mail: Luanjing.Guo@inl.gov

Key words: Reactive transport modeling; preconditioned Jacobian-free Newton-Krylov; urea hydrolysis; calcium carbonate precipitation

Summary. Multicomponent reactive transport systems in porous media that are large, highly nonlinear, and tightly coupled due to complex nonlinear reactions and strong solution-media interactions are often described by a system of coupled nonlinear partial differential algebraic equations (PDAEs). A preconditioned Jacobian-Free Newton-Krylov (JFNK) solution approach is applied to solve the PDAEs in a fully coupled, fully implicit manner. JFNK avoids explicitly computing and storing the Jacobian matrix during Newton nonlinear iterations allowing for efficient solution of coupled nonlinear systems. This solution approach is also enhanced by physics-based preconditioning and multigrid algorithms for efficient inversion of preconditioners. We have developed a reactive transport simulator named RAT based on this approach. Numerical results are presented to demonstrate the efficiency and massive scalability of the simulator for reactive transport problems involving strong solution-mineral interactions and fast kinetics. It has been applied to study the highly nonlinearly coupled reactive transport system of a promising *in situ* environmental remediation that involves urea hydrolysis and calcium carbonate precipitation.

1 INTRODUCTION

Reactive transport in porous media is a multiphysics problem in which fluid flow, solute transport, and biogeochemical reactions are all tightly coupled. Modeling reactive transport in porous media has many important applications, such as environmental remediation of contaminants in groundwater, geologic carbon sequestration and storage, underground nuclear waste disposal and recovery of geothermal energy. As reviewed by Yeh and Tripathi¹ and Steefel and MacQuarrie², three primary solution approaches exist, differing in the strategy chosen for coupling transport with reaction: (1) the global implicit approach (GIA), which solves all governing nonlinear equations simultaneously at each time step using various forms of Newton's method, (2) the sequential iteration approach (SIA), which subdivides the reactive transport problem into transport and reaction subproblems, solves them sequentially, and then iterates, and (3) the sequential non-iteration approach (SNIA), which solves the transport and reaction

problems sequentially without iteration, often referred as operator-splitting. The GIA was considered to be too CPU time and memory intensive¹ or to be computationally inefficient². Thus, in widely used reactive transport simulators, e.g. STOMP³, the operator-splitting approach has been implemented for its moderate computational resource requirement. However, when reactions and transport are tightly coupled, splitting error overwhelms solution accuracy leading to very small time steps¹.

In recent decades, advances in computing hardware and computational algorithms such as strongly convergent nonlinear solvers (including JFNK⁴) and efficient linear solvers such as Generalized Minimum Residual (GMRES)⁵, have made the fully coupled GIA approach attractive for reactive transport modeling⁶. In this paper, we present a massively parallel, multicomponent reactive transport simulator (RAT) that uses a preconditioned JFNK method to solve the system of nonlinear governing partial differential equations (PDEs) simultaneously. Its numerical performance is illustrated and its applicability to an *in situ* environmental remediation process of urea hydrolysis facilitated calcium carbonate precipitation in a column flow cell is presented.

2. PRECONDITIONED JACOBIAN-FREE NEWTON-KRYLOV METHOD

Newton's method for solving coupled nonlinear PDEs typically begins with a discrete form of the governing PDEs and casts it into a general residual function

$$\mathbf{F}(\mathbf{u}) = \mathbf{M}(\mathbf{u})\dot{\mathbf{u}} + \mathbf{K}(\mathbf{u})\mathbf{u} - \mathbf{R}(\mathbf{u}) = 0 \quad (1)$$

where \mathbf{u} is the solution vector, \mathbf{M} is the mass accumulation matrix, \mathbf{K} is the stiffness matrix (often with element values as functions of \mathbf{u}) and \mathbf{R} is the source term vector. $\mathbf{F}(\mathbf{u}): \mathbb{R}^1 \rightarrow \mathbb{R}^N$ is the system residual, where N is the number of unknowns. The Newton iterative method uses the full Jacobian matrix

$$\mathbf{J}(\mathbf{u}) = \frac{\partial \mathbf{F}(\mathbf{u})}{\partial \mathbf{u}} \quad (2)$$

to update the solution vector by solving the linearized system

$$\mathbf{J}(\mathbf{u}^{(k)})\delta\mathbf{u}^{(k)} = -\mathbf{F}(\mathbf{u}^{(k)}) \quad (3)$$

followed by an update of the solution state $\mathbf{u}^{(k+1)} = \mathbf{u}^{(k)} + \delta\mathbf{u}^{(k)}$. In the process, forming each element of \mathbf{J} can be difficult, time consuming and error-prone.

To solve this linear system, Krylov iterative solvers start with an initial guess of $(\delta\mathbf{u})_0$, forming initial linear residual, according to

$$\mathbf{r}_0 = -\mathbf{F} - \mathbf{J}(\delta\mathbf{u})_0 \quad (4)$$

Then the approximate solution of Eq. 3 at the l^{th} Krylov iteration is constructed from a linear

combination of the Krylov vectors $\{\mathbf{r}_0, \mathbf{J}\mathbf{r}_0, (\mathbf{J})^2\mathbf{r}_0, \dots, (\mathbf{J})^{l-1}\mathbf{r}_0\}$ constructed from the previous $l-1$ Krylov iterations,

$$(\delta\mathbf{u})_l = (\delta\mathbf{u})_0 + \sum_{j=0}^{l-1} \alpha_j (\mathbf{J})^j \mathbf{r}_0 \quad (5)$$

where the scalar coefficient α_j is part of the Krylov iteration⁵. Eq. 5 shows that the Krylov method for solving Eq. 3 only requires the product of the Jacobian matrix \mathbf{J} and Krylov vector \mathbf{v} , not the Jacobian itself. Specifically, to evaluate this matrix-vector product, $\mathbf{J}(\mathbf{u}^{(k)})\mathbf{v}$, a finite difference approach, Eq. 6, can be used⁴, where ε is a very small perturbation.

$$\mathbf{J}(\mathbf{u}^{(k)})\mathbf{v} \approx \frac{\mathbf{F}(\mathbf{u}^{(k)} + \varepsilon\mathbf{v}) - \mathbf{F}(\mathbf{u}^{(k)})}{\varepsilon} \quad (6)$$

The use of preconditioning in solving the linear system of Eq. 3 is to efficiently cluster eigenvalues of the iteration matrix, which in turn will reduce the number of Krylov iterations required for convergence. When applying the right preconditioning to Eq. 3, one solves

$$(\mathbf{J}(\mathbf{u}^{(k)})\mathbf{P}^{-1})(\mathbf{P}\delta\mathbf{u}^{(k)}) = -\mathbf{F}(\mathbf{u}^{(k)}) \quad (7)$$

where \mathbf{P} is a linear operator and symbolically represents the preconditioning process. \mathbf{P} is chosen in the manner such that it is a suitable approximation to the Jacobian matrix. The right preconditioned version of the JFNK matrix-vector product approximation of Eq. 6 becomes

$$(\mathbf{J}(\mathbf{u}^{(k)})\mathbf{P}^{-1})\mathbf{v} \approx \frac{\mathbf{F}(\mathbf{u}^{(k)} + \varepsilon\mathbf{P}^{-1}\mathbf{v}) - \mathbf{F}(\mathbf{u}^{(k)})}{\varepsilon} \quad (8)$$

Thus the preconditioned JFNK process is implemented in two steps: 1) Solve $\mathbf{P}\mathbf{y} = \mathbf{v}$ for \mathbf{y} ; 2) Perform matrix-vector product approximation using Eq. 8; and repeat steps 1 and 2 until the Krylov iteration converges.

In a physics-based preconditioning approach, the preconditioner \mathbf{P} is not obtained by algebraically manipulating the Jacobian matrix; rather, approximations are made to the original differential system to form a Jacobian system for preconditioning purpose. We illustrate a general implementation of the physics-based preconditioning for reactive transport below.

Following Lichtner⁷, the general PDEs that govern reactive transport read as

$$\frac{\partial}{\partial t} \theta(c_l + \underbrace{\sum_{m=1}^{N_c} v_{lm} K_{eq,m} \prod_{n=1}^{N_c} c_n^{v_{nm}}}_{\text{equilibrium reaction}}) + \underbrace{(-\nabla \theta \mathbf{D} \cdot \nabla + \mathbf{q} \cdot \nabla)(c_l + \sum_{m=1}^{N_c} v_{lm} K_{eq,m} \prod_{n=1}^{N_c} c_n^{v_{nm}})}_{\text{transport}} - \underbrace{\sum_{k=1}^{N_c} \theta b_{lk} R_k(c_1, \dots, c_{N_c})}_{\text{kinetic reaction}} \quad (9)$$

$l = 1, 2, \dots, N_c$

Detailed notations can be found in our related publication⁸. The weak form of Eq. 9 is

$$\begin{aligned}
 & \left(\frac{\partial}{\partial t} \theta(c_l + \sum_{m=1}^{N_s} v_{lm} K_{eq,m} \prod_{n=1}^{N_c} c_n^{v_{nm}}), \phi_i \right) - \left(\theta \mathbf{D} \cdot \nabla(c_l + \sum_{m=1}^{N_s} v_{lm} K_{eq,m} \prod_{n=1}^{N_c} c_n^{v_{nm}}), \nabla \phi_i \right) \\
 & + \left(\mathbf{q} \nabla(c_l + \sum_{m=1}^{N_s} v_{lm} K_{eq,m} \prod_{n=1}^{N_c} c_n^{v_{nm}}), \phi_i \right) - \left(\sum_{k=1}^{N_k} \theta b_{lk} R_k(c_1, \dots, c_{N_c}), \phi_i \right) = 0, \quad l = 1, N_c
 \end{aligned} \tag{10}$$

where ϕ_i is the finite element basis function, and $(,)$ represents the inner product and integration over the domain. One can cast the weak form into a residual function and take the derivative with respect to the concentration c_l to obtain the analytical Jacobian, which could be used as the preconditioning matrix \mathbf{P} . It can be further simplified to have only lower and diagonal (L+D) blocks or only the diagonal blocks (D) as

$$\mathbf{P} \approx \begin{bmatrix} \mathbf{J}_{11} & \mathbf{0} & \cdots & \mathbf{0} \\ \mathbf{J}_{21} & \mathbf{J}_{22} & \cdots & \mathbf{0} \\ \vdots & \vdots & \ddots & \vdots \\ \mathbf{J}_{N_c,1} & \mathbf{J}_{N_c,2} & \cdots & \mathbf{J}_{N_c,N_c} \end{bmatrix} \quad \text{or} \quad \mathbf{P} \approx \begin{bmatrix} \mathbf{J}_{11} & \mathbf{0} & \cdots & \mathbf{0} \\ \mathbf{0} & \mathbf{J}_{22} & \cdots & \mathbf{0} \\ \vdots & \vdots & \ddots & \vdots \\ \mathbf{0} & \mathbf{0} & \cdots & \mathbf{J}_{N_c,N_c} \end{bmatrix} \tag{11}$$

In our implementation of preconditioned JFNK, the full preconditioning matrix is never actually formed. For the L+D case, the preconditioning process $\mathbf{y} = \mathbf{P}^{-1} \mathbf{v}$ per Krylov iteration per Newton iteration is done via the following steps:

1. Approximate the inversion of a linear system to solve for \mathbf{y}_1 from

$$\mathbf{J}_{11} \mathbf{y}_1 = \mathbf{v}_1 \tag{12}$$

2. Approximate the inversion of a linear system to solve for \mathbf{y}_2 from

$$\mathbf{J}_{22} \mathbf{y}_2 = \mathbf{v}_2 - \mathbf{J}_{21} \mathbf{y}_1 \tag{13}$$

Repeat Step 2 until the last row block \mathbf{y}_{N_c} is solved. Then pass \mathbf{y} to the Krylov iteration Step 2 descrito perform matrix-vector product approximation (Eq. 8).

3. MOOSE PARALLEL COMPUTING FRAMEWORK AND RAT SIMULATOR

We implemented methodologies described in the previous section in RAT, a finite element based parallel simulator for modeling multicomponent reactive transport in porous media. RAT is built upon a parallel Multiphysics Object Oriented Simulation Environment (MOOSE) computational framework developed at Idaho National Laboratory⁹. Figure 1(a) shows a strong scaling test of the simulator ranging from 640 to 10240 processors. The result indicates the close-to-ideal scaling performance. In Figure 1(b), it is shown that effective preconditioners enhance the linear solver convergence and further increase the numerical efficiency of the simulator.

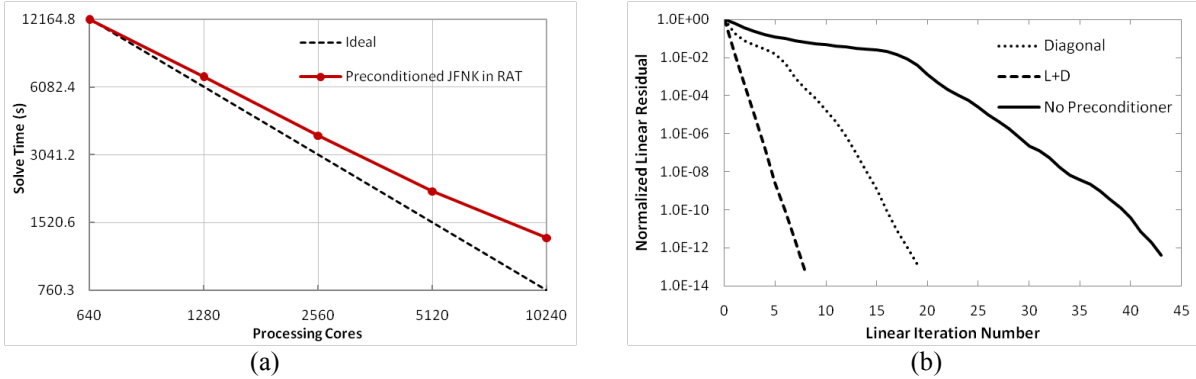


Figure 1 Numerical efficiency and parallel performance of RAT: (a) strong scaling on a distributed memory parallel system, and (b) linear solver performance with various preconditioning strategies.

4 APPLICATIONS AND RESULTS DISCUSSION

We applied RAT to model a system of ureolytically driven calcium carbonate precipitation, which has been studied as a way to immobilize radionuclide contaminants *in situ* through coprecipitation in subsurface^{10,11}. In flow column lab tests, both urea and calcium solutions are injected into the flow column. Bicarbonate ions are produced in the zone where urease enzyme presents and react with injected calcium solution to form CaCO_3 precipitates. This system involves kinetic aqueous urea hydrolysis, kinetic CaCO_3 precipitation/dissolution reactions, and equilibrium aqueous speciation reactions. The simplified reaction network shown in Table 1 is considered in our simulations.

Equilibrium Reaction	Keq	Equilibrium Reaction	Keq
$H^+ + HCO_3^- \Leftrightarrow CO_2(aq)$	6.341	$-H^+ + HCO_3^- \Leftrightarrow CO_3^{2-}$	-10.325
$-H^+ + Ca^{2+} + HCO_3^- \Leftrightarrow CaCO_3(aq)$	-7.009	$Ca^{2+} \Leftrightarrow H^+ + CaOH^+$	-12.85
$Ca^{2+} + HCO_3^- \Leftrightarrow CaHCO_3^+$	1.043	$-H^+ + NH_4^+ \Leftrightarrow NH_3(aq)$	-9.492
$-H^+ + SiO_2 \Leftrightarrow SiO_2 - OH$	-10.0	$-H^+ \Leftrightarrow OH^-$	-13.991
Kinetic Reaction			
$Ca^{2+} + HCO_3^- \Leftrightarrow H^+ + CaCO_3(s) \quad R_{Calcite} = -A \cdot k_{ref} \cdot e^{\frac{-E_a}{R} \left(\frac{1}{T} - \frac{1}{T_{ref}} \right)} \left[1 - \frac{C_{Ca^{2+}} \cdot C_{HCO_3^-} \cdot (C_{H^+})^{-1}}{K_{eq}} \right]$			
$Urea \xrightleftharpoons{Urease} 2NH_4^+ + HCO_3^- + OH^- \quad R_{ureolysis} = C_{urease} \cdot \frac{k_{ref}^U \cdot e^{\frac{-E_a^U}{R} \left(\frac{1}{T} - \frac{1}{T_{ref}^U} \right)} \cdot C_{urea}}{(K_M + C_{urea}) \cdot \left(1 + \frac{C_{NH_4^+} + C_{NH_3(aq)}}{K_p} \right) \cdot \left(1 + \frac{C_{H^+}}{K_{ES,1}} + \frac{K_{ES,2}}{C_{H^+}} \right)}$			

Table 1 Reaction network considered for the ureolytic calcite precipitation system⁸ (equilibrium constants are 10 based values from the EQ3/6 database¹²).

4.1 Urea Hydrolysis Analysis

The flow column is being modeled as a one-dimensional system with the injection concentration of urea and calcium at 0.03 mol/L. The urease enzyme is attached to the porous medium within a zone from 0.16 m to 0.33 m. We performed sensitivity studies of the effects of flow rate and the immobilized enzyme concentration on the spatiotemporal distribution of mineral precipitates. Four combinations of different flow rate and urease concentration are considered: (1) low flow rate (QL) of 5 mL/min and high urease concentration (uH) of $C_{urease} = 15.445 \text{ g/L}$; (2) high flow rate (QH) of 10 mL/min and high urease concentration (uH) of $C_{urease} = 15.445 \text{ g/L}$; (3) low flow rate (QL) of 5 mL/min and low urease concentration (uL) of $C_{urease} = 0.3089 \text{ g/L}$; and (4) high flow rate (QH) of 10 mL/min and low urease concentration (uL) of $C_{urease} = 0.3089 \text{ g/L}$.

Figure 2(a) shows urea concentration profiles. It is clear that urea only hydrolyzes where urease enzyme presents, and when urease concentration is high (uH cases), more urea hydrolyzed (more declination in the profile). pH is a critical factor impacting the distribution of precipitation. It is determined by three competing processes: urea hydrolysis, calcite precipitation, and hydroxide sorption to solid surface. Urea hydrolysis tends to increase the pH, while calcite precipitation tends to reduce it. In addition, the sorption of hydroxide to the medium surface also has lead to the increase of hydrogen concentration due to the enormous sorption capacity of the selected chromatographic material. The resulting pH profiles are shown in Figure 2(b). As soon as urea starts to hydrolyze at the head of the enzyme zone, pH increases. The ureolysis rate determines the overall maximum value of pH the system gets. The higher the enzyme concentration is, the higher the maximum pH value gets. Downstream from the ureolysis zone, pH decreases drastically because only pH-reducing mechanisms take place in this region.

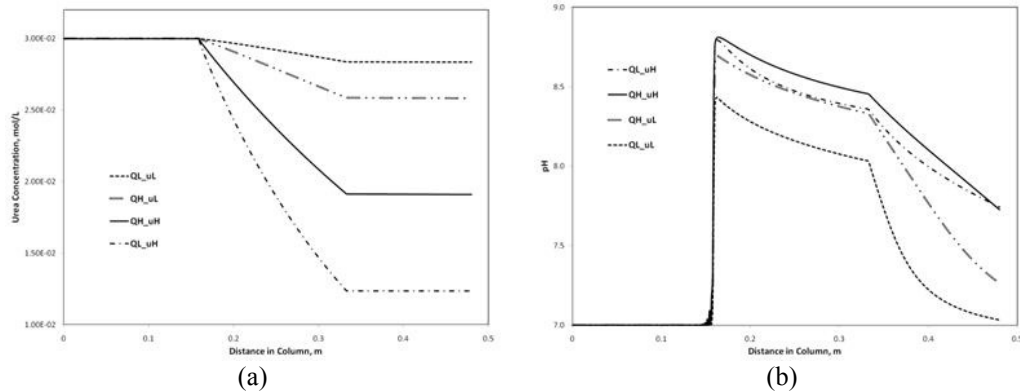


Figure 2 Concentration profiles along the column for (a) urea, and (b) pH at various scenarios.

4.2 Calcium Carbonate Precipitation Analysis

The profiles of CaCO_3 concentration (moles of precipitates per volume of solution) along the column at different pore volumes of fluid being injected are shown in Figure 3. Some general

conclusions can be drawn. Firstly, for all four combinations of flow rate and urease concentration, the calcite precipitation occurred primarily within the urea hydrolysis zone. At the end of this zone, an abrupt drop in the profiles takes place. Secondly, urease concentration is the overall dominating factor on the amount of precipitates. The higher concentration of urease enzyme leads to larger ureolysis rate and more calcite precipitation. Thirdly, as time progresses, the amount of precipitates increases. Lastly, beyond the enzyme zone, precipitation reaction continues due to excess Ca^{2+} and HCO_3^- ions being transported downstream. The steep slopes in the dropping profiles indicate a relatively fast precipitation reaction.

When urease concentration is high (Figure 3(a)), there is a distinct difference in the spatial distribution of CaCO_3 between the high flow rate and low flow rate scenarios. Larger amount of precipitates were formed with low flow rate due to longer residence time. In the low flow rate case, precipitates focus at the head of the enzyme zone; and more uniformly along the urease zone at a higher flow rate. The reason is that when flow is slow, the system is transport limited. Once bicarbonate is produced, it gets into the solid phase, leading to a narrow and focused precipitation zone. As flow rate is increased, the system becomes more reaction limited, resulting in more uniformly distributed solid. For the lower enzyme concentration scenarios (Figure 3(b)), there is only slight difference in the spatial distribution patterns of mineral phase. More precipitates were formed as a consequence of the longer residence time in low flow rate case. The precipitation rate for both cases is mainly limited by the supply of bicarbonate ion. As the excess bicarbonate ion accumulates along the reaction zone, the amount of precipitates grows.

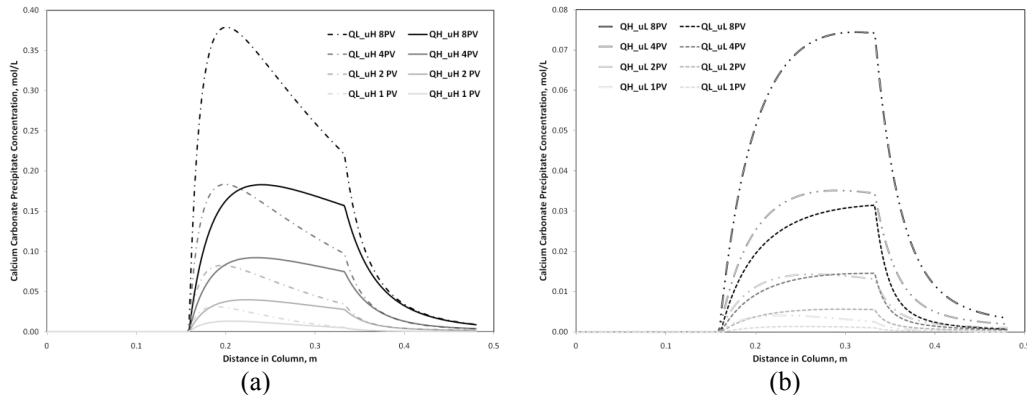


Figure 3 Distribution of calcium carbonate precipitates along the column at 1, 2, 4 and 8 pore volumes of injection for different combination of flow rate and enzyme concentration.

5 CONCLUSIONS

Through MOOSE, we developed a JFNK based nonlinear solution approach for general purpose multi-dimensional reactive transport modeling. Successful application of three numerical algorithms lead to an efficient solution capability: the Newton-Krylov nonlinear solver, the physics-based preconditioning, and algebraic multigrid. The efficiency and scalability of this solution approach were demonstrated through examples involving strong solution-mineral interactions and fast kinetics. We have routinely applied the diagonal preconditioner and

achieved satisfactory preconditioning performance even for highly nonlinear reactive transport problems. Hence, the preconditioned JFNK approach can be very efficient even for large, highly nonlinear reactive transport problems. Applying the simulator of RAT to a complex reactive transport system of ureolytically driven calcium carbonate precipitation, it has provided insights into understand the nonlinear coupling effects between various processes.

REFERENCES

- [1]. Yeh, G.T. and V.S. Tripathi, *A Critical-Evaluation of Recent Developments in Hydrogeochemical Transport Models of Reactive Multichemical Components* Water Resources Research, 1989. **25**(1): p. 93-108,
- [2]. Steefel, C.I. and K.T.B. MacQuarrie, *Approaches to modeling of reactive transport in porous media*. Reviews in Mineralogy and Geochemistry, 1996. **34**: p. 83-129,
- [3]. White, M.D. and B.P. McGrail, *STOMP (Subsurface Transport Over Multiple Phase) Version 1.0 Addendum: ECKEChem Equilibrium-Conservation-Kinetic Equation Chemistry and Reactive Transport*, in Report PNNL-15482. 2005, Pacific Northwest National Laboratory, Richland, Washington.
- [4]. Knoll, D.A. and D.E. Keyes, *Jacobian-free Newton-Krylov methods: a survey of approaches and applications*. Journal of Computational Physics, 2004. **193**(2): p. 357-397, doi:10.1016/j.jcp.2003.08.010.
- [5]. Saad, Y. and M.H. Schultz, *GMRES - A Generalized Minimal Residual Algorithm for Solving Nonsymmetric Linear-Systems*. Siam Journal on Scientific and Statistical Computing, 1986. **7**(3): p. 856-869,
- [6]. Hammond, G.E., A.J. Valocchi, and P.C. Lichtner, *Application of Jacobian-free Newton-Krylov with physics-based preconditioning to biogeochemical transport*. Advances in Water Resources, 2005. **28**(4): p. 359-376, doi:10.1016/j.advwatres.2004.12.001.
- [7]. Lichtner, P.C., *Continuum formulation of multicomponent-multiphase reactive transport*. Reviews in Mineralogy and Geochemistry, 1996. **34**: p. 1-81,
- [8]. Guo, L., H. Huang, D. Gaston, C. Permann, D. Andrs, G. Redden, C. Lu, D. Fox, and Y. Fujita, *A Parallel, Fully Coupled, Fully Implicit Solution to Reactive Transport in Porous Media Using the Preconditioned Jacobian-Free Newton-Krylov Method*. Advances in Water Resources, Submitted,
- [9]. Gaston, D., C. Newman, G. Hansen, and D. Lebrun-Grandie, *MOOSE: A parallel computational framework for coupled systems of nonlinear equations*. Nuclear Engineering and Design, 2009. **239**(10): p. 1768-1778, doi:10.1016/j.nucengdes.2009.05.021.
- [10]. Warren, L.A., P.A. Maurice, N. Parmar, and F.G. Ferris, *Microbially mediated calcium carbonate precipitation: Implications for interpreting calcite precipitation and for solid-phase capture of inorganic contaminants*. Geomicrobiology Journal, 2001. **18**(1): p. 93-115,
- [11]. Fujita, Y., J.L. Taylor, T.L.T. Gresham, M.E. Delwiche, F.S. Colwell, T.L. McLing, L.M. Petzke, and R.W. Smith, *Stimulation of microbial urea hydrolysis in groundwater to enhance calcite precipitation*. Environmental Science & Technology, 2008. **42**(8): p. 3025-3032, doi:10.1021/es702643g.
- [12]. Wolery, T.J., *EQ3/6, A Software Package for Geochemical Modeling of Aqueous Systems: Package Overview and Installation Guide (Version 7.0)*, in Report UCRL-MA-110662 PT I. 1992, Lawrence Livermore National Laboratory: Livermore, CA.